

# TRANSVERSE MAGNETIC WAVES IN MYELINATED NERVES

M. M<sup>a</sup> Villapece<sup>1</sup>, L. M<sup>a</sup> Roa<sup>2</sup>, and J. Reina-Tosina<sup>1</sup>

<sup>1</sup>Área de Teoría de la Señal y Comunicaciones, E.S. de Ingeniería, University of Seville, Seville, Spain  
<sup>2</sup> Biomedical Engineering Group, E.S. de Ingeniería, University of Seville, Seville, Spain

**Abstract-** The structure of myelinated axons is quite similar to that of a high-loss coaxial cable. An electromagnetic analysis of TM waves shows that distributed effects cannot be neglected. The attenuation and phase constants are obtained as a function of frequency. Predicted finite wave delay in the internodal segment approaches measurements.

**Keywords -** Nerves, models, electromagnetism, waves, velocity, delay, attenuation, myelin

## I. INTRODUCTION

Electric stimulation of nervous system can restore motor functions [1]. Electrical properties of nerves are usually described by means of a cable model [2], [10]. This model is frequently simplified, and each internodal segment is modeled by a lumped impedance. This can be a series resistor [3]-[7], but sometimes parallel capacitive impedances are added [27]. A lumped resistor is unable to model a finite conduction velocity in the internodal segment, whereas the presence of capacitors modelling the myelin sheath can explain delays [27]. Despite this fact, resistor models are more frequently used, and the delay is usually assigned only to nonlinearities in Ranvier nodes [15].

The existence of travelling waves in internodal segments could linearly explain, at least partially, the measured conduction speed [14]. The objective of this paper is to determine whether under any circumstances a distributed circuit [28] covering the effects of both the capacitive and resistive effects would be more suitable than a lumped model. To answer this question we shall analyze an internodal segment through which a transverse magnetic (TM) wave is guided [20], [26]. This approach links with the spatially distributed description of electric and magnetic fields found in literature [7], [11]-[13], [18], [19].

From an electromagnetic point of view, lumped element models are obtained as a quasi-static approximation [20]. Clark *et al.* [21] calculate the wave number  $k$  as

$$k = \omega \sqrt{\mu_0 \epsilon (1 + \sigma / j\omega \epsilon)} \quad (1)$$

For axoplasm at 1kHz with conductivity 5 mhos/m, the resultant wave number approximates 0.198 rad/m. In 10 cm., the phase shift is less than 0.02 radian or 1.46°, so in [21] conclude the field is quasi-static. This conclusion was later adopted explicitly [22] or implicitly in lumped element models [3]-[7], [27]. We shall show that the waves are not defined by  $k$ , but rather by the propagation constant  $h$ , and that quasi-static approximations don't apply always, specially for relatively high frequencies.

## II. METHODOLOGY

For sake of simplicity, we shall consider an infinitely long segment, surrounded by an infinite extracellular medium. Even though the results will not be the same found in physiological situations, qualitative conclusions might be useful to gain understanding into nerve conduction. The structure is quite similar to a high-loss coaxial cable (fig. 1). Medium 1 is the axoplasm, medium 2 is the myelin sheath, and medium 3 is the extracellular fluid.

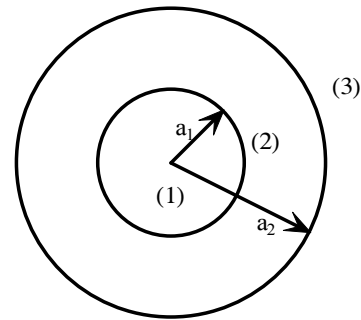


Fig. 1. Myelinated nerve coaxial model. Axon radius is  $a_1$  and fiber radius is  $a_2$ .

We shall assume isotropic, homogeneous and linear media [11]-[13],[16]-[18], although the physiologic medium in which the nerve is embedded is neither isotropic [8]-[9] nor homogeneous [4]. The myelin sheath is sometimes considered as a perfect insulator [3], [7], [18]. We don't assume this hypothesis [27]. All media will be generic with permittivity  $\epsilon_i$ , permeability  $\mu_0$ , and conductivity  $\sigma_i$ , where subscript  $i$  refers to medium 1, 2 or 3. Let the media be charged due to present ions. When these ions come into the axon at Ranvier nodes, they diffuse [23], and thus a diffusion current appears. Therefore, the current density  $\mathbf{J}$  at any point designed by  $\mathbf{r}$  in any media, when an electric field  $\mathbf{E}$  dependent on frequency  $\omega$  appears can be expressed as [24]:

$$\mathbf{J}(\mathbf{r}, \omega) = \sigma \mathbf{E}(\mathbf{r}, \omega) - \sum_i D_i \nabla \rho_i(\mathbf{r}, \omega) \quad (2)$$

where the sum extends to all present ions ( $Na^+; K^+; Cl^- \dots$ ) [23] and  $D_i$  is the diffusion constant of ion  $i$ . The ionic diffusion would exist even if the ions were uncharged particles [24].

The magnetic field intensity  $\mathbf{H}$  is solenoidal and may, therefore, be derived from the curl of a suitable Hertzian vector potential  $\mathbf{\Pi}_e$  [25], [26]:

## Report Documentation Page

<b>Report Date</b> 25OCT2001	<b>Report Type</b> N/A	<b>Dates Covered (from... to)</b> -
<b>Title and Subtitle</b> Transverse Magnetic Waves in Myelinated Nerves	<b>Contract Number</b>	
	<b>Grant Number</b>	
	<b>Program Element Number</b>	
<b>Author(s)</b>	<b>Project Number</b>	
	<b>Task Number</b>	
	<b>Work Unit Number</b>	
<b>Performing Organization Name(s) and Address(es)</b> Área de Teoría de la Señal y Comunicaciones, E.S. de Ingeniería, University of Seville, Seville, Spain	<b>Performing Organization Report Number</b>	
<b>Sponsoring/Monitoring Agency Name(s) and Address(es)</b> US Army Research, Development & Standardization Group (UK) PSC 802 Box 15 FPO AE 09499-1500	<b>Sponsor/Monitor's Acronym(s)</b>	
	<b>Sponsor/Monitor's Report Number(s)</b>	
<b>Distribution/Availability Statement</b> Approved for public release, distribution unlimited		
<b>Supplementary Notes</b> Papers from the 23rd Annual International Conference of the IEEE Engineering in Medicine and Biology Society, 25-28 October 2001, held in Istanbul, Turkey. See also ADM001351 for entire conference on cd-rom.		
<b>Abstract</b>		
<b>Subject Terms</b>		
<b>Report Classification</b> unclassified	<b>Classification of this page</b> unclassified	
<b>Classification of Abstract</b> unclassified	<b>Limitation of Abstract</b> UU	
<b>Number of Pages</b> 4		

$$\mathbf{H} = j\omega\epsilon_{eq}\nabla \times \mathbf{\Pi}_e \quad (3)$$

where

$$\epsilon_{eq} = \epsilon_0\epsilon_r - j\frac{\sigma}{\omega} \quad (4)$$

Substitution of (3) into Faraday's law and subsequent integration leads to

$$\mathbf{E} = k^2\mathbf{\Pi}_e + \nabla\phi \quad (5)$$

where  $k$  was defined in (1) and  $\phi$  is an arbitrary scalar potential function. Using (1) in Ampère-Maxwell's law,

$$\nabla \times \mathbf{H} = j\omega\epsilon_{eq}\mathbf{E} - \sum_i D_i \nabla \rho_i \quad (6)$$

Substituting (3) into (6) we find that

$$\nabla \times \nabla \times \mathbf{H} = k^2\mathbf{\Pi}_e + \nabla\phi - \sum_i \frac{D_i \nabla \rho_i}{j\omega\epsilon_{eq}} \quad (7)$$

Since  $\phi$  is yet an arbitrary function, we propose the following gauge:

$$\phi = \nabla \cdot \mathbf{\Pi}_e + \sum_i \frac{D_i \rho_i}{j\omega\epsilon_{eq}} \quad (8)$$

Hence an homogeneous wave equation is obtained for  $\mathbf{\Pi}_e$ . Let's adopt a cylindrical coordinates system axially centered in the axon  $(r, \theta, z)$ . The wave equation reduces to

$$\nabla^2 \mathbf{\Pi}_e + k^2 \mathbf{\Pi}_e = 0 \quad (9)$$

Despite the existence of a diffusion current, the election of the gauge given by (8) makes this equation to be the same as if the media were uncharged. Transverse magnetic modes may be derived from  $\mathbf{\Pi}_e = \pi_e \mathbf{z}$ , thus assuming  $\mathbf{\Pi}_e$  have no other components but the axial. The solution to wave equation (9) is [25]:

$$\mathbf{\Pi}_e = \sum_{n=0}^{\infty} \frac{1}{\lambda_n^2} a_n \psi_n \mathbf{z} \quad (10)$$

where  $a_n$  is an amplitude constant and  $\psi_n$  is a space and frequency dependent function given by

$$\psi_n = Z_n(\lambda_n r) e^{-jn\theta} e^{-jh_n z} \quad (11)$$

in which  $Z_n(\lambda_n r)$  is a generic Bessel function of order  $n$ . By definition,

$$\lambda_n = \sqrt{k^2 - h_n^2} \quad (12)$$

In these equations,  $h_n = \beta_n - j\alpha_n$  is the propagation constant, inherently different to  $k$ . Phase constant is  $\beta_n$  (rad/m) and  $\alpha_n$  is the attenuation constant (Np/m). We shall proof that the thickness of the axon myelin sheath is much less than the wavelength of physiological signals, so that the asymmetric modes (dependent on  $\theta$ , and thus with  $n \neq 0$ ) are evanescent [25] and attenuate quickly ( $\beta_n=0$ ). Therefore, the main mode has  $n=0$  and the fields will correspondingly be denoted  $\mathbf{E}_0$  and  $\mathbf{H}_0$ . The electric field can be obtained using (8) and (10) in (5):

$$E_{0r} = -\frac{j h_0}{\lambda_0^2} a_0 \frac{\partial \psi_0}{\partial r} + j\omega\mu \frac{1}{k^2} \sum_i D_i \frac{\partial \rho_i}{\partial r} \quad (13)$$

$$E_{0\theta} = j\omega\mu \frac{1}{k^2} \sum_i D_i \frac{1}{r} \frac{\partial \rho_i}{\partial \theta} \quad (14)$$

$$E_{0z} = a_0 \psi_0 + j\omega\mu \frac{1}{k^2} \sum_i D_i \frac{\partial \rho_i}{\partial z} \quad (15)$$

The magnetic field is found from (3):

$$H_{0r} = 0 \quad (16)$$

$$H_{0\theta} = -\frac{jk^2}{\mu\omega\lambda^2} a_0 \frac{\partial \psi_0}{\partial r} \quad (17)$$

$$H_{0z} = 0 \quad (18)$$

Note the absence of axial component in the magnetic field in this propagation mode, despite the diffusion current. This is therefore a TM mode [26]. At  $r=0$  the field must be finite so  $Z_0^{(1)} = J_0$ , with  $J_0$  the Bessel function of the first kind and order 0. In the external fluid, the field can not increase with distance and should behave like a travelling wave; therefore  $Z_0^{(3)} = H_0^{(1)}$ , where  $H_0$  is the Hankel function. In the myelin sheath,  $Z_0^{(2)} = J_0 + c_0 N_0$ , with  $N_0$  the Bessel function of the second kind and order 0, and  $c_0$  a constant to be determined.

Boundary conditions for the continuity of  $E_z$  and  $H_\theta$  at  $r=a_1$  y  $r=a_2$  lead to an inhomogeneous equations set for  $a_0^{(1)}$ ,  $a_0^{(2)}$ ,  $c_0 a_0^{(2)}$  and  $a_0^{(3)}$ . For the system to have more than a single solution, and allow waveguiding happen independently of charge gradient, the determinant of this set of equations must vanish. The determinantal equation is the same that can be found for uncharged media [25]:

$$\frac{\lambda_2 k_1^2 J_1(\lambda_2 a_1) N_0(\lambda_2 a_1) - \lambda_1 k_2^2 J_0(\lambda_1 a_1) N_1(\lambda_2 a_1)}{\lambda_2 k_1^2 J_1(\lambda_1 a_1) J_0(\lambda_2 a_1) - \lambda_1 k_2^2 J_0(\lambda_1 a_1) J_1(\lambda_2 a_1)} - \frac{\lambda_2 k_3^2 H_1^{(1)}(\lambda_3 a_2) N_0(\lambda_2 a_1) - \lambda_3 k_2^2 H_0^{(1)}(\lambda_3 a_2) N_1(\lambda_2 a_2)}{\lambda_2 k_3^2 H_1^{(1)}(\lambda_3 a_2) J_0(\lambda_2 a_1) - \lambda_3 k_2^2 H_0^{(1)}(\lambda_3 a_2) J_1(\lambda_2 a_2)} = 0 \quad (19)$$

The roots of equation (9) together with (12) are the propagation constants  $h_{0m}$ , with  $m=1,2,3,\dots$

### III. RESULTS

The electrical properties of media shown in Fig. 1 can be found in Table I. We are interested only in  $h_{01}$ , since higher modes present stronger attenuation. Figs. 2 and 3 show the the phase constant  $\beta$  and the attenuation constant  $\alpha$  as a function of frequency. Frequency values have been chosen so as to cover the whole spectrum of physiological signals.

Signal velocity can be calculated as  $\omega/\beta$  (fig. 4). Wavelengths are determined as  $2\pi/\beta$  (see Table II).

TABLE I  
ELECTRICAL PROPERTIES OF MYELINATED NERVE MEDIA

Parameter	Symbol	Value	Unit	Reference
Axoplasm Conductivity	$\sigma_1$	0.909	S/m	[29]
Myelin Conductivity	$\sigma_2$	3.45e-6	S/m	[30]
External Conductivity	$\sigma_3$	0.333	S/m	[31]
Axoplasm Permittivity	$\epsilon_1$	$\epsilon_0$	F/m	
Myelin Permittivity <sup>a</sup>	$\epsilon_2$	$25.5\epsilon_0$	F/m	
External Permittivity	$\epsilon_3$	$\epsilon_0$	F/m	
Axon Radium <sup>aa</sup>	$a_1$	6.2	$\mu\text{m}$	
Fiber Radium	$a_2$	10	$\mu\text{m}$	[23]

<sup>a</sup>Derived from coaxial capacity  $5e-3 \mu\text{F}/\text{cm}^2$  [10], [24]

<sup>aa</sup>Using  $2a_1 = 0.8 \times 2a_2 - 1.8$  [32]

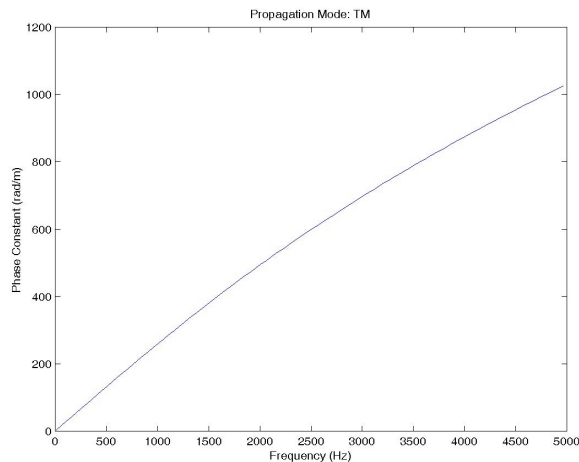


Fig. 2. Phase constant as a function of frequency

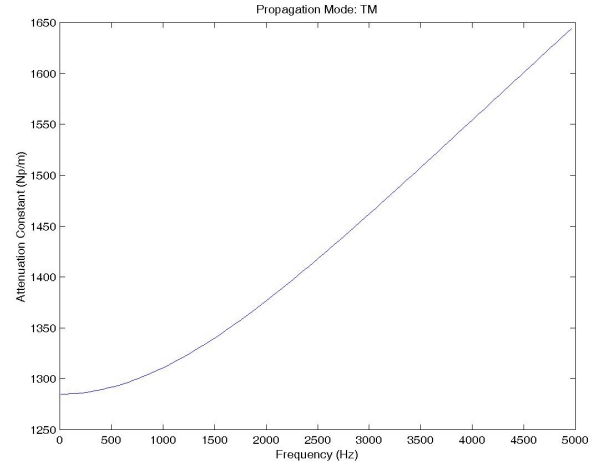


Fig. 3. Attenuation constant as a function of frequency.

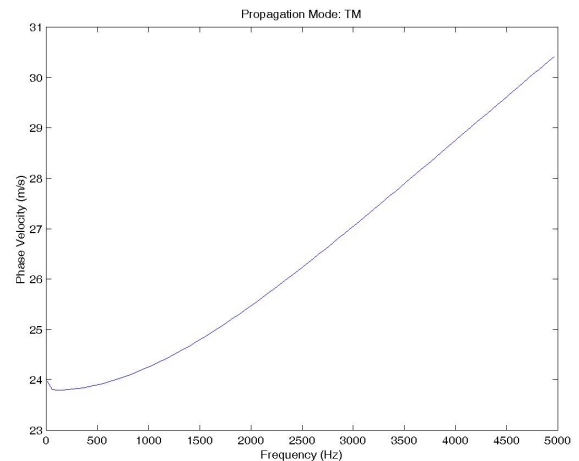


Fig. 4. Wave velocity as a function of frequency.

### IV. DISCUSSION

Phase constant is, at 1kHz, higher than 200rad/m (125.6° in 10cm). This value is far away from 0.198 rad/m pointed out by Clark *et al.* [21], [22] and shows the need for a distributed parameter model. Note that, as one could expect, this is more true as frequency increases. Therefore, the nerve behaviour is not always quasi-static. Wavenumber and propagation constant are the same when the wave is TEM [26], but we are dealing with TM modes. Attenuation constant is more or less constant at frequencies below 250 Hz, and then increases linearly. For a typical internodal distance of 1 mm [23], low frequency signals attenuate up to 0.28 times their value, despite their frequency. At higher frequencies, attenuation grows approximately at a 3 dB/decade rate.

The order of magnitude of concerning wavelengths are a thousand times greater than the thickness of the myelin sheath, validating a previous assumption.

Signal velocity is independent of frequency up to 500 Hz. Values are similar to those measured in [33] (25-41 m/s), [14]. Therefore delay is not only due to Ranvier nodes, but also to internodal segments. This result is in agreement with [27], but no we have used no lumped element.

Equation (2) is an extension of Ohm's law. Lumped element circuits neglect the diffusion current, taking into account only the drift current due to the electric field. But ionic diffusion would be present even in absence of axial electric field.

TABLE II  
WAVELENGTHS IN MYELINATED NERVES

Frequency (Hz)	Wavelength (mm)
50	396
100	216
500	46
1000	24
2500	10
5000	6

### V. CONCLUSION

Whereas lumped circuit models are much easier to deal with, the quasi-static hypothesis doesn't hold for relatively high frequencies and a distributed model might be more adequate. TM waves linearly model attenuation and non-zero delay in the internodal segment, and could help to gain more insight into neural artificial stimulation problems. Further research is required to analyze other propagation modes.

### ACKNOWLEDGMENT

The authors wish to thank Dr. J. Ribas, MD. for his suggestions.

### REFERENCES

[1] R. B. Stein, P. H. Peckman, and D. B. Popovic, *Neural Prosthesis: Replacing Motor Function After Disease or Disability*. New York: Oxford Univ. Press, 1992.  
 [2] N. H. Sabah, "Aspects of nerve conduction," *IEEE Eng. Med. Biol. Mag.*, vol. 19, no. 6, 2000, pp. 111-118.  
 [3] D. R. McNeal, "Analysis of a model for excitation of myelinated nerve," *IEEE Trans. Biomed. Eng.*, vol. BME-23, pp. 329-337, 1976.  
 [4] A. Q. Choi, J. K. Cavanaugh, and D. M. Durand, "Selectivity of multiple-contact nerve cuff electrodes: a simulation analysis," *IEEE Trans. Biomed. Eng.*, vol. 48, pp. 165-172, Feb. 2001.  
 [5] N. J. M. Rijkhoff, J. Holsheimer, F. M. J. Debruyne, and H. Wijkstra, "Modelling selective activation of small myelinated fibres using a monopolar point electrode," *Med. & Biol. Eng. & Comput.*, vol. 33, pp. 762-768, 1995.  
 [6] V. Schnabel, and J. J. Struijk, "Magnetic and electrical stimulation of undulating nerve fibres: a simulation study," *Med. & Biol. Eng. & Comput.*, vol. 37, pp. 704-709, 1999.  
 [7] C. M. Zierhofer, "Analysis of a linear model for electrical stimulation of axons - critical remarks on the activating function concept," *IEEE Trans. Biomed. Eng.*, vol. 48, pp. 173-184, Feb. 2001.  
 [8] W. M. Grill, Jr., "Modeling the effects of electric fields on nerve fibers: influence of tissue electrical properties," *IEEE Trans. Biomed. Eng.*, vol. 46, pp. 918-928, Aug. 1999.

[9] R. B. Szlavik, "The effect of anisotropy on the potential distribution in biological tissue and its impact on nerve excitation simulations," *IEEE Trans. Biomed. Eng.*, vol. 47, pp. 1202-1210, Sep. 2000.  
 [10] P. J. Basser, "Cable equation for a myelinated axon derived from its microstructure," *Med. & Biol. Eng. & Comput.*, vol. 31, pp. S87-S92, 1993.  
 [11] S. S. Nagarajan, D. M. Durand, and E. N. Warman, "Effects of induced electric fields on finite neuronal structures: a simulation study," *IEEE Trans. Biomed. Eng.*, vol. 40, no. 11, pp. 1175-1188, Nov. 1993.  
 [12] F. Rattay, "Analysis of models for external stimulation of axons," *IEEE Trans. Biomed. Eng.*, vol. BME-33, no. 10, pp. 974-977, Oct. 1986.  
 [13] F. Rattay, "Analysis of models for extracellular fiber stimulation," *IEEE Trans. Biomed. Eng.*, vol. 36, no. 7, pp. 676-682, Feb. 1989.  
 [14] M. D. Wells, "A method to improve the estimation of conduction velocity distributions over a short segment of nerve," *IEEE Trans. Biomed. Eng.*, vol. 46, pp. 1107-1120, Sep. 1999.  
 [15] B. Frankenhaeuser, and A. F. Huxley, "The action potential in the myelinated fiber of *Xenopus Laevis* as computed in the basis of voltage clamp data," *J. Physiol. (London)*, vol. 171, p.302, 1964.  
 [16] P. J. Basser, R. S. Wijesinghe, and B. J. Roth, "The activating function for magnetic stimulation derived from a three-dimensional volume conductor model," *IEEE Trans. Biomed. Eng.*, vol. 39, no. 11, pp. 1207-1210, Nov. 1992.  
 [17] P. J. Basser, "Focal magnetic stimulation of an axon," *IEEE Trans. Biomed. Eng.*, vol. 41, no. 6, pp. 601-606, June 1994.  
 [18] E. N. Warman, W. M. Grill, and D. Durand, "Modeling the effects of electric fields on nerve fibers: determination of excitation thresholds," *IEEE Trans. Biomed. Eng.*, vol. 39, no. 12, pp. 1244-1254, Dec. 1992.  
 [19] K. P. Esselle, and M. A. Stuchly, "Neural stimulation with magnetic fields: analysis of induced electric fields," *IEEE Trans. Biomed. Eng.*, vol. 46, no. 7, pp. 693-700, July 1992.  
 [20] S. Ramo, J. R. Whinnery, and T. Van Duzer, *Fields and Waves in Communication Electronics*, 3rd ed., New York: John Wiley & Sons, 1994.  
 [21] J. Clark, and R. Plonsey, "A mathematical evaluation of the core conductor model," *Biophys. J.*, vol. 6, no. 1, pp. 95-112, 1966.  
 [22] J. K. Woosley, B. J. Roth, and J. P. Wikswo, Jr., "The magnetic field of a single axon: a volume conductor model," *Math. Bioscience*, no. 76, pp. 1-36, 1985.  
 [23] V. Schnabel, and J. J. Struijk, "Calculation of electric fields in a multiple cylindrical volume conductor induced by magnetic coils," *IEEE Trans. Biomed. Eng.*, vol. 48, no. 1, pp. 78-86, Jan. 2001.  
 [24] C. R. Noback, and R. J. Demarest, *The human nervous system: basic principles of neurobiology* McGraw Hill, 1975.  
 [25] M. Zahn, *Electromagnetic field theory: a problem solving approach*, New York: John Wiley & Sons, 1979.  
 [26] J. A. Stratton, *Electromagnetic theory*, New York: McGraw-Hill Co., 1941.  
 [27] R. E. Collin, *Field theory of guided waves*, 2nd ed., Piscataway: IEEE Press & Oxford University Press, 1990.  
 [28] A. G. Richardson, C. C. McIntyre, W. M. Grill, "Modelling the effects of electric fields on nerve fibres: influence of the myelin sheath," *Med. Biol. Eng. Comput.*, vol. 38, pp. 438-446, 2000.  
 [29] M. M<sup>a</sup> Villapeccellin-Cid, L. M<sup>a</sup> Roa-Romero, L. J. Reina-Tosina, "Transmission line based model for electronic propagation in myelinated nerves," *MEDICON*, Croatia, 2001.  
 [30] R. Stampfli, "Bau und funktion isolierter markhaltiger nervenfaseren," *Ergeb. Physiol.*, vol. 47, p. 70, 1952.  
 [31] I. Tasaki, "New measurements of the capacity and the resistance of the myelin sheath and the nodal membrane of the isolated frog nerve fiber," *Amer. J. Physiol.*, vol. 181, p. 639, 1955.  
 [32] C. Abzug, M. Maeda, B. W. Peterson, and V. J. Wilson (with an Appendix by C. P. Bean), "Cervical branching of lumbar vestibulospinal axons," *J. Physiol. (London)*, vol. 115, p. 101, 1951.  
 [33] W. A. Wessellink, J. Holsheimer, and H. B. K. Boom, "A model of the electrical behaviour of myelinated sensory nerve fibres based on human data," *Med. Biol. Eng. Comput.*, vol. 37, pp. 228-235, 1999.  
 [34] G. Schalow, G. A. Zäch, and R. Warzok, "Classification of human peripheral nerve fiber groups by conduction velocity and nerve fiber diameter is preserved following spinal cord lesion," *J. Aut. Nervous Syst.*, vol. 52, pp. 125-150, 1995.